IEEE TRANSACTIONS ON

INTELLIGENT TRANSPORTATION SYSTEMS

A PUBLICATION OF THE IEEE INTELLIGENT TRANSPORTATION SYSTEMS SOCIETY

JULY 2016 VOLUME 17 NUMBER 7 ITISFG (ISSN 1524-9050)

(Contents Continued on Back Cover)

IEEE

(Contents Continued from Front Cover)

SHORT PAPERS

GUEST EDITORIAL

SPECIAL ISSUE PAPERS

Integrated Longitudinal and Lateral Control for Kuafu-II Autonomous Vehicle

Linhai Xu, Yingzhou Wang, Hongbin Sun, *Member, IEEE*, Jingmin Xin, *Senior Member, IEEE*, and Nanning Zheng, *Fellow, IEEE*

***Abstract*—Over the past decades, there has been significant research effort dedicated to the development of autonomous vehicles and advanced driver assistance systems. The driving control system, which is responsible for trajectory tracking and driving safety, is one of the most important technologies for autonomous vehicles. This paper describes the design of driving control system, including both longitudinal and lateral controllers, for the Kuafu-II autonomous vehicle. Compared with most of the previous researches that inevitably require a large amount of parameters, the presented control system design in this paper integrates several typical and efficient controllers to significantly reduce the system sensitivity to these parameters, and it is able to achieve the system robustness under diversified circumstances. The effectiveness of the presented control system design has been extensively evaluated under simulation and on road tests.**

***Index Terms*—Autonomous vehicle, longitudinal control, lateral control, trajectory tracking.**

I. Introduction

As one of the most fascinating technology trends in automotive industry, autonomous vehicle is expected to make significant impact on the future improvement of traffic safety and transport efficiency. Therefore, autonomous vehicle has attracted great attention from academic and industry communities. In DARPA Grand Challenge [1] and Urban Challenge [2] held in 2004, 2005 and 2007 respectively, hundreds of teams from all over the world participated to compete and demonstrate their technology achievements on autonomous vehicle. In addition, since 2009 National Natural Science Foundation of China (NSFC) has organized annual competition named "Intelligent Vehicle Future Challenge (IVFC)" [3] to push forward the related technology and academic research in China. This paper describes automatic driving control system design of Kuafu-II autonomous vehicle as shown in Fig. 1, which is based on Chery Tiggo compact crossover and has been evaluated in the competition of Intelligent Vehicle Future Challenge.

In general, the autonomous vehicle integrates environment perception, planning and automatic driving modules [4]–[6].

Fig. 1. The Kuafu-II autonomous vehicle.

The automatic driving module manipulates the corresponding actuators according to the requirement of planning module, and guarantee that vehicle moves at the desired speed profile and path trajectory. Hence, the performance of automatic driving control system is critical to the safety and stability of autonomous vehicle. The automatic driving control system for autonomous vehicle includes both longitudinal and lateral controllers. The longitudinal controller is responsible for regulating the velocity of vehicle according to the speed requirement, while the lateral controller manipulates the steering system of vehicle for trajectory tracking. The integration of longitudinal and lateral control is able to further improve the dynamics and lateral stability of autonomous vehicle.

Both longitudinal and lateral controllers have been exploited in the driving control system of autonomous vehicle during the past few decades. Initially, longitudinal and lateral controllers designed by using zero-pole placement were studied at the Ohio State University [7]. In California PATH program, Ioannou *et al.* used an adaptive controller as an intelligent cruise controller [8]. Hingwe and Tomizuka proposed a sliding mode control for lateral control [9]. Hedrick *et al.* proposed to use the optimal preview Frequency Shaped Linear Quadratic control for lateral controller and the sliding mode control for longitudinal controller respectively [10]. In AUTOPIA program, Naranjo *et al.* designed a fuzzy-logic-based longitudinal controller to maintain a reference velocity or keep a safe distance from other vehicles [11]. Meanwhile, lateral control that is responsible for steering and trajectory tracking attracts more attention. Joshu Prez designed a cascade architecture to emulate a human driver's behavior and further improve the performance of lateral controller [12]. The combination or coupling of longitudinal and lateral control has also been exploited and

Manuscript received March 15, 2015; revised August 2, 2015; accepted August 7, 2015. Date of publication November 23, 2015; date of current version June 24, 2016. This work was supported by the Key Program of National Natural Science Foundation of China under Grant 91120308. The Associate Editor for this paper was L. Li.

The authors are with the Institute of Artificial Intelligence and Robotics, Xi'an Jiaotong University, Xi'an 710049, China (e-mail: xlh@mail.xjtu.edu.cn).

Color versions of one or more of the figures in this paper are available online at http://ieeexplore.ieee.org.

Digital Object Identifier 10.1109/TITS.2015.2498170

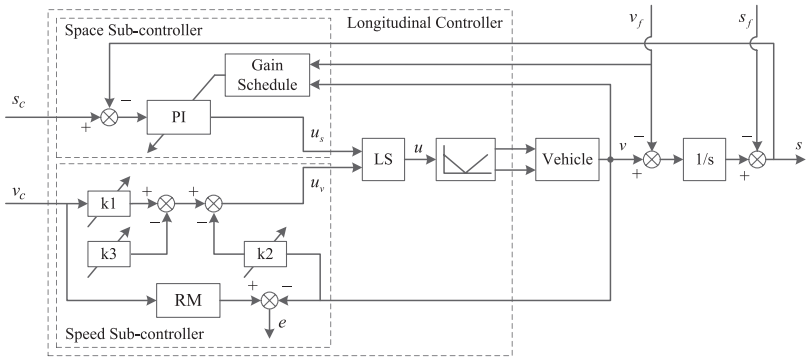

Fig. 2. Block diagram of longitudinal control algorithm.

considered as an effective way to further improve the lateral stability and vehicle dynamics [13], [14]. Moreover, the design of overall driving control systems in autonomous vehicles is also extensively discussed to present control algorithm from system level [4]–[6], [15], [16]. In particular, Autonomous Audi TTS was designed to enable the operations at the limits of friction [17].

The implemented driving control system in Kuafu-II autonomous vehicle integrates longitudinal and lateral controllers. The longitudinal controller is designed as a override structure, which employs a gain schedule PI to guarantee safe headway and a model reference adaptive system to track speed profile. The lateral controller includes nonlinear feedback proportional control and sliding control to improve the tracking accuracy in different speed grades. The longitudinal and lateral controllers are further integrated together to achieve robust trajectory tracking and automatic parking according to path planning. Compared with most of previous researches that inevitably require a large amount of parameters, the presented control system design in this paper integrates several typical and efficient controllers to significantly reduce the system sensitivity to these parameters, and it is able to achieve the system robustness under diversified circumstances. The control system has been implemented and integrated in Kuafu-II autonomous vehicle, and its performance has been demonstrated by simulation and on road test. Equipped with the described control system, Kuafu-II autonomous vehicle has participated in Intelligent Vehicle Future Challenge and won the second prize in 2012.

The rest of this paper is organized as follows: Section II describes the vehicle modeling and control laws exploited in Kuafu-II vehicle. Section III presents the system design and vehicle setup. The experimental results and evaluation are extensively discussed in Sections IV and V. Finally, Section VI concludes this paper.

II. Vehicle Modeling and Control Laws

The aim of our work is not to exploit any new models, instead is just based on several existing models. We choose these models and corresponding control methods in order to improve compatibility of the presented driving control system by minimizing calibration. Although there are many methods of tracking desired trajectory, ranging from a slow speed maneuver to a limits handling maneuver. As a platform to verify robotic perception and planning, Kuafu-II autonomous vehicle should be controlled fully at slow speed, and it should be controlled in small signal range at high speed without the limit maneuver.

A. Longitudinal Control

The longitudinal controller aims to track the desired speed profile specified by planning system while retaining safe headway for vehicle. It has two command inputs, i.e., the safe distance headway s_c depending on time headway and current speed, the desired speed v_c specified by the planning system. The longitudinal controller outputs two control signals to directly manipulate two actuators, including throttle and brake pedal, which are used to regulate the speed of vehicle and keep safe headway.

The structure of the proposed longitudinal controller is shown in Fig. 2. Because the throttle and brake pedal are not allowed to be activated simultaneously, we use one control signal to manipulate the two actuators in the fashion of split range. The longitudinal controller employs an override control structure to combine the speed and space sub-controllers. In normal condition, the speed sub-controller has the priority to be used. While, when an obstacle appears on the planned trajectory and poses a threat to the headway, the space sub-controller has the priority to take its function. By making the speed sub-controller adopt reverse action while the space sub-controller adopt direct action, a low selector (LS) can be used to construct the override controller. The design of speed and space sub-controllers will be introduced respectively in details in this section.

The powertrain, composed by the engine, transmission and drivetrain, presents a complicated nonlinear relation from the throttle to the speed of the vehicle. The analysis of validated nonlinear powertrain model and our empirical experience reveal that the plant can be approximated as a first-order system around a operating point. By neglecting the dynamics between brake command and braking torque because it is much more faster than the dynamics of vehicle inertial, the plant from braking command to the speed of vehicle can also be regarded as a first-order system around a operating point dominated by the Newton's laws. The operating point is affected by those factors such as road condition, aerodynamic drag, and vehicle mass changes that are treated as disturbances.

By simplifying the plant as a first-order, time-variant system, the speed sub-controller is designed as a model reference adaptive controller. The simplified longitudinal vehicle model is shown as

$$\dot{v} = -av + bu + d \tag{1}$$

where the unknown parameters a, b, and d vary with road condition, aerodynamic drag, vehicle speed, etc.

The desired response is given by the reference model defined as Eqn. (2)

$$\dot{v}_m = -a_m v_m + b_m v_c \tag{2}$$

where $a_m > 0$ and b_m are specified according to the response speed, riding quality, etc.

Let the controller given by

$$u_v = k_1 v_c - k_2 v - k_3. \tag{3}$$

The perfect model-following will be achieved by $k_1 = b_m/b$, $k_2 = (a_m - a)/b$, $k_3 = d/b$.

The stable adaptation law is derived by using Lyapunov's stability theory. We take the deviation signal $e = v - v_m$, then the derivative of the e is written as:

$$\frac{de}{dt} = \dot{v} - \dot{v}_m = -a_m e - (a - a_m + bk_2)v + (bk_1 - b_m)v_c + (d - bk_3). \tag{4}$$

Then we have the Lyapunov function and its derivative as:

$$L(e, k_1, k_2, k_3) = \frac{1}{2}\left(e^2 + \frac{1}{b\gamma}(a - a_m + bk_2)^2 + \frac{1}{b\gamma}(bk_1 - b_m)^2 + \frac{1}{b\gamma}(d - bk_3)^2\right) \tag{5}$$

$$\frac{dL}{dt} = -a_m e^2 + \frac{1}{\gamma}(a - a_m + bk_2)\left(\frac{dk_2}{dt} - \gamma v e\right) + \frac{1}{\gamma}(bk_1 - b_m)\left(\frac{dk_1}{dt} + \gamma v_c e\right) + \frac{1}{\gamma}(d - bk_3)\left(\gamma e - \frac{dk_3}{dt}\right). \tag{6}$$

By adopting the adaptation law

$$\begin{cases} \frac{dk_1}{dt} = -\gamma v_c e \\ \frac{dk_2}{dt} = \gamma v e \\ \frac{dk_3}{dt} = -\gamma e \end{cases} \tag{7}$$

and bounding the parameters k_1, k_2, k_3 and deviation e, we guarantee the deviation $e \to 0$ when $t \to \infty$.

For the space sub-controller, the command input is specified by $s_c = s_0 + hv$, where h is time headway and s_0 is minimum distance. As shown in Fig. 2, the space sub-controller take a PI control law with a gain schedule. The current speed of vehicle and the relative speed between vehicle and obstacle are used as scheduling variables. The PI controller is tuned for several operating conditions, which are high relative speed at high speed, low relative speed at high speed, and low speed respectively. A narrow proportional band is adopted for high speed, while a wide proportional band for low speed. A weak integral action, used to cope the disturbance, such as road conditions, should be tuned to ensure the response is over-damped.

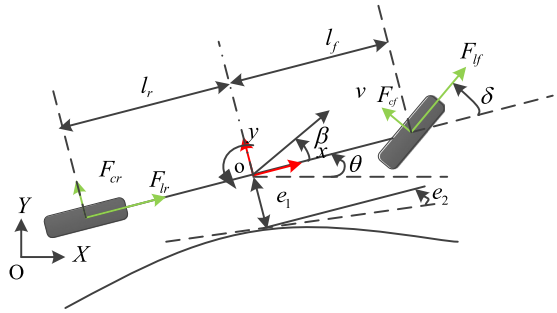

Fig. 3. Bicycle model of the vehicle.

As a widely-used industrial technique, the global stability of override control structure can be guaranteed by carefully tuning. Theoretically, the override control structure with a low-selector (LS) can be transformed into an equivalent single loop system consisting of one non-linear and one linear subsystems, to which the standard input/output stability theory, such as circle criterion, is applicable [18], [19]. In our practice implementation, while the speed sub-controller is bypass by the low-selector, the adaption law should be deactivated.

B. Lateral Control

The lateral controller is used to track the desired trajectory that is generated by the planning system. The input of lateral controller includes cross-track error, orientation error and their derivatives, which can be calculated by using the position and pose of vehicle from the perception module and the desired trajectory from the planning module. The output of lateral controller is the commands to steering actuators.

The lateral characteristic of vehicle is depicted as a bicycle model (shown in Fig. 3) based on the following assumptions:

1) The vehicle is treated as a rigid body, and the dynamics of suspension is neglected;
2) The dynamics between steering wheel and front wheels is omitted, and steering system is regarded as a fixed gain;
3) The two wheels of each axle are lumped into one wheel in the centerline of the vehicle;
4) The vehicle moves on a flat road and we neglect the force analysis along vertical direction.

We denote inertial coordinate as XOY, and coordinate fixed on vehicle as xoy whose origin is located at CG (Centre of Gravity) of the vehicle.

While the vehicle travel at low speed, the lateral force of the wheels with rubber tire can be neglected. We can focus on the kinematic characteristic of the vehicle. By using the kinematic model, we get the slip angle of CG

$$\beta = \arctan\left(\frac{l_r \tan\delta}{l_f + l_r}\right) \tag{8}$$

and the instantaneous curvature of CG

$$\kappa = \frac{\tan\delta\cos\beta}{l_f + l_r}. \tag{9}$$

When the vehicle travels at high speed, the effect of the lateral force can not be neglected. Considering the lateral force as linear proportional to the slip angle of wheel, we get a simple dynamic model. Defining state variable as $\mathbf{x_g} = [y, \dot{y}, \theta, \dot{\theta}]^{\mathrm{T}}$, we get the bicycle dynamic model shown as

$$\dot{\mathbf{x}}_g = \begin{bmatrix} 0 & 1 & 0 & 0 \\ 0 & \frac{-2C_f\cos\delta - 2C_r}{mv_x} & 0 & \frac{-2C_f l_f\cos\delta + 2C_r l_r}{mv_x} - v_x \\ 0 & 0 & 0 & 1 \\ 0 & \frac{-2C_f l_f\cos\delta + 2C_r l_r}{I_z v_x} & 0 & \frac{-2C_f l_f^2\cos\delta - 2C_r l_r^2}{I_z v_x} \end{bmatrix} \mathbf{x}_g + \begin{bmatrix} 0 \\ \frac{2C_f\cos\delta}{m} \\ 0 \\ \frac{2C_f l_f\cos\delta}{I_z} \end{bmatrix} \delta \tag{10}$$

where $\dot{y}$ is vehicle velocity along the lateral principle axis of the vehicle, $\dot{\theta}$ is yaw rate of the vehicle, m is mass of the vehicle, I_z is yaw moment of inertia of the vehicle, C_f and C_r are cornering stiffness of the front and rear tires, l_f and l_r are distances of the front axle and rear axle from CG of the vehicle, v_x is vehicle velocity along the longitudinal principle axis of the vehicle, and δ is steering angle.

An effective and simple steering control law for the lateral controller used by Stanley, the winner of DARPA Grand Challenge, is shown as:

$$\delta(t) = e_2(t) + \arctan\frac{ke_1(t)}{v_x(t)} \tag{11}$$

where $e_1(t)$ denotes cross-track error, $e_2(t)$ is orientation error, and k is gain parameter, which determines convergence rate. Here, the reference point used to calculate cross-track error $e_1(t)$ is located at CG of the vehicle. This slightly differs from Stanley's law that is located at the center of front axle.

As a nonlinear feedback proportional control law, this simple controller works well for lower speeds (less than 10 m/s). However, it neglects the important dynamics of the vehicle, such as mass and yaw moment, and assumes the ideal tires with infinite stiffness. With speed increase, the performance of the controller degrades seriously. In Stanley, a series of offset that is calibrated and verified in testing, is imposed to compensate these effects. With our approach, a SMC (sliding mode control) is used to cope the dynamics in high speed and the model imprecision.

In order to design the sliding mode controller, we further simplified the dynamics characteristic of the bicycle model by making two assumptions:

1) When the vehicle is in high speed, the steering behavior is limited so that when high speed driving, the δ is small enough to approximate $\cos(\delta)$ to be 1;
2) The longitudinal velocity and the curvature of trajectory are regarded as constants approximately, in order to get the acceleration of the desired yaw angle to be zero ($\ddot{\theta}_{\mathrm{des}} \approx 0$).

Then, by rewritten state variable as $\mathbf{e} = [e_1, \dot{e}_1, e_2, \dot{e}_2]^{\mathrm{T}}$, where e_1 and e_2 are cross-track error and orientation error respectively, the dynamics of vehicle is presented as

$$\dot{\mathbf{e}} = \begin{bmatrix} 0 & 1 & 0 & 0 \\ 0 & \frac{-2C_f-2C_r}{mv_x} & \frac{2C_f+2C_r}{m} & \frac{-2C_f l_f+2C_r l_r}{mv_x} \\ 0 & 0 & 0 & 1 \\ 0 & \frac{-2C_f l_f+2C_r l_r}{I_z v_x} & \frac{2C_f l_f-2C_r l_r}{I_z} & \frac{-2C_f l_f^2-2C_r l_f^2}{I_z v_x} \end{bmatrix} \mathbf{e} + \begin{bmatrix} 0 \\ \frac{-2C_f l_f+2C_r l_r}{mv_x} - v_x \\ 0 \\ \frac{-2C_f l_f^2-2C_r l_r^2}{I_z v_x} \end{bmatrix} \dot{\theta}_{\mathrm{des}} + \begin{bmatrix} 0 \\ \frac{2C_f}{m} \\ 0 \\ \frac{2C_f l_f}{I_z} \end{bmatrix} \delta. \tag{12}$$

The observation taken from a preview point in front of the vehicle can be acquired by $e_o = e_1 + d\sin(e_2)$. When the orientation error e_2 is small, we can further get

$$e_o \approx e_1 + de_2 \tag{13}$$

where d is the distance between CG(center of gravity) of the vehicle and the preview point in front of the vehicle.

The plant used to design the sliding mode controller is depicted as

$$\begin{aligned} \ddot{e}_o &= \ddot{e}_1 + d\ddot{e}_2 = f(x) + b\delta \\ &= (f_1(x) + df_2(x)) + (b_1 + db_2)\delta \end{aligned} \tag{14}$$

where

$$\begin{aligned} f_1(x) =& -\frac{2C_f + 2C_r}{mv_x}\dot{e}_1 + \frac{2C_f + 2C_r}{m}e_2 \\ & - \frac{2C_f l_f - 2C_r l_r}{mv_x}(\dot{e}_2 + \dot{\theta}_{\mathrm{des}}) - v_x\dot{\theta}_{\mathrm{des}} \end{aligned} \tag{15}$$

$$\begin{aligned} f_2(x) =& -\frac{2C_f l_f - 2C_r l_r}{I_z v_x}\dot{e}_1 + \frac{2C_f l_f - 2C_r l_r}{I_z}e_2 \\ & - \frac{2C_f l_f^2 + 2C_r l_f^2}{I_z v_x}(\dot{e}_2 + \dot{\theta}_{\mathrm{des}}) \end{aligned} \tag{16}$$

$$b_1 = \frac{2C_f}{m} \tag{17}$$

$$b_2 = \frac{2C_f l_f}{I_z}. \tag{18}$$

We obtain $\hat{f}(x)$ and $\hat{b}$, which are estimations of $f(x)$ and b, by using the parameters listed in Table. I. The imprecision of the parameters m, I_z, C_f, C_r, l_f, l_r are bounded by$|\hat{f(x)} - f(x)| \le F$, $|\hat{b} - b| \le B$.

By defining the sliding surface as

$$s = \dot{e}_o + 2\lambda e_o + \lambda^2 \int_0^t e_o(\tau)d\tau \tag{19}$$

we get the control law

$$\delta = \hat{b}^{-1}\left(-\hat{f} - 2\lambda\dot{e}_o - \lambda^2 e_o - k\cdot\mathrm{sat}\left(\frac{s}{\phi}\right)\right) \tag{20}$$

TABLE I
VEHICLE MODEL PARAMETERS

Parameter	Notation	Value
Vehicle mass	m	1600 kg
Vehicle yaw moment	I_z	3000 kgm^2
Front-CG distance	l_f	1.1 m
Rear-CG distance	l_r	1.4 m
Cornering stiffness of front tires	C_f	80000 $Nrad^{-1}$
Cornering stiffness of rear tires	C_r	80000 $Nrad^{-1}$

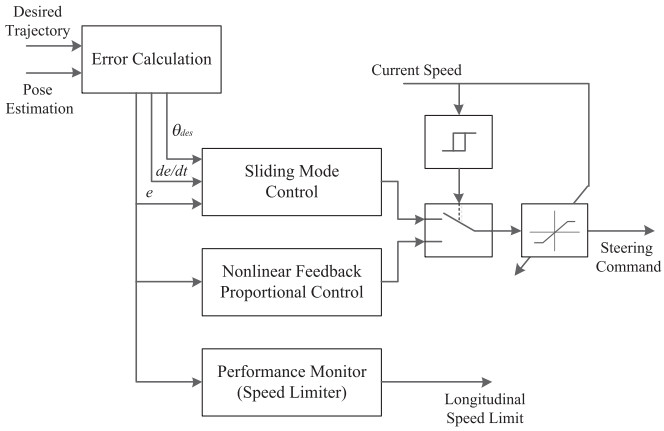

Fig. 4. Block diagram of lateral control algorithm.

where

$$k \geq \beta(F+\eta) + (\beta-1)|-\hat{f} - \lambda \dot{e}_o|$$

$$\beta = \left(\frac{b_{\max}}{b_{\min}}\right)^{\frac{1}{2}}$$

$$\text{sat}\left(\frac{s}{\phi}\right) = \begin{cases} 1 & s > \phi \\ s & -\phi \leq s \leq \phi \\ -1 & s < -\phi \end{cases}$$

which ensures $s\dot{s} \leq -\eta|s|$, $\eta > 0$. The proper k should be chosen carefully that guarantee to result $s = 0$ after some time and keep on the surface after that.

Fig. 4 illustrates the structure of lateral controller, which includes two steering sub-controllers, i.e. a sliding mode controller and a nonlinear feedback proportional controller, which are combined by a selector. The selector is controlled by the current speed of the vehicle. A dedicated performance monitor is used to monitor the quality of sliding mode control. When the tracking performance worsens, the performance monitor will require the vehicle to slow down. In addition, when the vehicle speed is below a certain threshold, the lateral controller will be switched to Stanley's law from the sliding mode control. To prevent the frequent switching between these two sub-controllers, a Schmitt trigger has been exploited. Finally, to prevent the dangerous, threatening and abnormal behaviors of the vehicle when autonomous running, the permissible steering command is also limited by the vehicle speed. This is quite similar to human driving, where only small magnitude steering commands can be applied when the vehicle speed is high. To achieve this, a clamper is exploited, whose upper and lower bounds are regulated by the current speed of the vehicle.

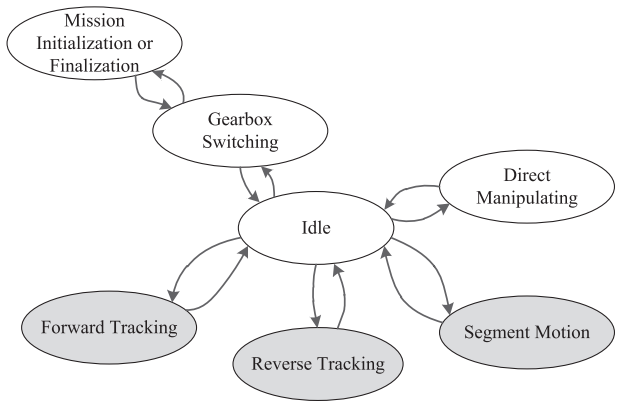

Fig. 5. Finite state machine of the driving control.

C. Integration of Longitudinal and Lateral Control

The longitudinal controller and the lateral controller should be integrated for various driving states of the autonomous vehicle. Kuafu-II autonomous vehicle employs a finite state machine to manage various driving states. As shown in Fig. 5, the proposed finite state machine includes 7 states, i.e., Mission initialization or finalization, Idle, Gearbox switching, Forward tracking, Reverse tracking, Segment motion, and Direct manipulating.

In Forward tracking state, the vehicle is required to track the planned trajectory. In order to use different environment-expressing formats from different inputs, the planned trajectory is expressed as a sequential set of points. For the purpose of error calculation, the parameterized cubic spline interpolation function is used to generate the desired trajectory that is smooth and continuous. The chord length is used as the parameter of cubic spline interpolation function. When tracking the desired trajectory, the aforementioned longitudinal controller and lateral controller are integrated in the fashion that longitudinal regulation has higher priority. For a gentle human driver, when the attitude of the vehicle deviates from the expectation obviously, deceleration is his first reaction. Accordingly, the use of performance monitor in the lateral controller guarantees the slowing down of vehicle when the deviation increase obviously. Together with the effects of the clamper in lateral controller, to integrate longitudinal and lateral controllers in this manner can effectively enhance safety although it may restrict maneuverability at high speed.

When the lateral and longitudinal controllers have been integrated, couple will occur between these controllers. The integration of both controllers constructs a semi-couple system, in which the longitudinal controller is not affected by the lateral controller, but the lateral controller is sensitive to the longitudinal speed regulation. In the case of low speed, the stability of the non-linear proportional lateral controller has been verified by proving the error converges exponentially to zero using a bicycle model with infinite tire stiffness and tight steering

limitations [4]. In the case of high speed, the stability of slide mode control is guaranteed by ensuring $s\dot{s} \leq -\eta|s|, \eta > 0$. But in practical, the longitudinal dynamic characteristic has affected by steering because tire traction force has been decomposed. However, the first-order time-variant assumption is applicable, the adaptive algorithm can still effectively eliminate its effect.

In Reverse tracking state, the manner to integrate longitudinal and lateral controllers is largely similar to that in Forward tracking state. The only difference is that the vehicle speed in this state is relatively low, so that the slide mode control in lateral controller will not be activated.

Segment motion state is mainly used for vehicle parking, where vehicle is controlled to move along the specified segments, such as arc and line. In this state, longitudinal controller is employed to achieve a velocity profile, and the lateral controller should be bypassed and the steering command is generated from the reverse kinematic model.

Besides longitudinal and lateral controllers, several auxiliary controllers are also employed in other driving states. These auxiliary controllers are mainly in charge of the position of gear lever and the force on braking pedal.

In Gearbox switching state, a position controller is employed to operate gear lever actuator to switch among Parking, Reverse, and Driving, and a torque controller is employed to ensure that a sufficient force has been applied on the braking pedal to keep the autonomous vehicle still. Please note that this torque controller are also employed in Idle state.

Direct manipulating state is used to permit decision making and planning module to directly manipulate steering wheel, braking pedal and throttle. This state is an abnormal state where steering wheel and pedal actuators are changed to be controlled by upper level modules in position mode.

Mission initialization and finalization state is a special state, in which no control function is activated. The autonomous vehicle keeps still by placing gear lever in Parking position. This state is used as the start and end for all autonomous missions.

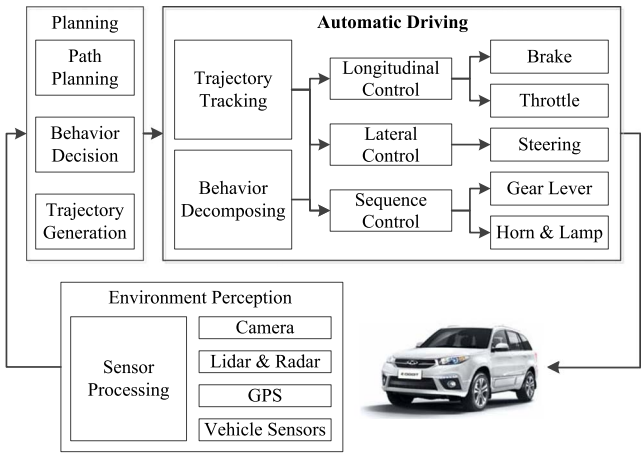

Fig. 6. Overall control architecture of Kuafu-II autonomous vehicle.

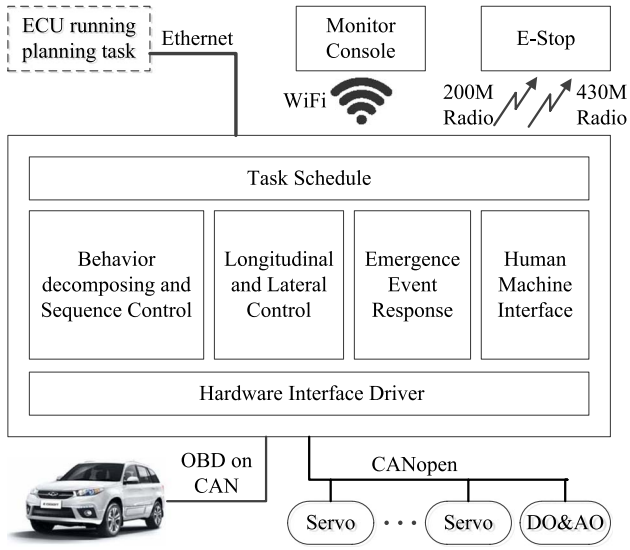

Fig. 7. Hardware and software implementation of proposed control system.

III. System Design and Vehicle Setup

Fig. 6 illustrates the overall control architecture of Kuafu-II autonomous vehicle which generally consists of three major modules, i.e., environment perception, planning and automatic driving. The employed sensors on Kuafu-II vehicle include Lidar, Radar, GPS, cameras and other vehicle sensors. The environment perception module processes the input data from diversified sensors and generates the symbolic description of traffic environment for the following planing and driving control modules. The planning module accomplishes the path planning, behavior decision and trajectory generation. The automatic driving module controls the vehicle according to the commands of planning module. It firstly converts the desired trajectory and the driving behavior into longitudinal and lateral controller, and it further operates the corresponding actuators, including brake, throttle, steering, gear lever, horn and lamps.

The hardware and software implementations of the proposed driving control system are illustrated in Fig. 7. The overall automatic driving module is implemented on an industrial PC, which receives planning commands through Ethernet from another computer that runs decision making and planning tasks. The driving module connects to the vehicle by OBD (On Board Diagnostics) on CAN (Control Area Network), to acquire the vehicle status. By using CANopen bus, it interacts with servo drivers, digital and analog I/O devices to control brake, throttle, etc. For status monitoring and manual intervention, the driving module also connects with a monitoring console by WiFi network. It is supervised by E-stop (Emergency Stop) by using dedicated 200 M / 430 M redundant radio link. The major part in software is longitudinal and lateral control programs, which operate servo drivers, DO and AO devices by using hardware interface drivers. In addition, behavior decomposing and sequence control, emergence event response and human machine interface run concurrently with the control program by multi-task scheduling on Linux operating system.

To drive the vehicle automatically, several actuators have been installed to be operated by computers. Fig. 8 shows the actuators and computing system installed on Kuafu-II vehicle,

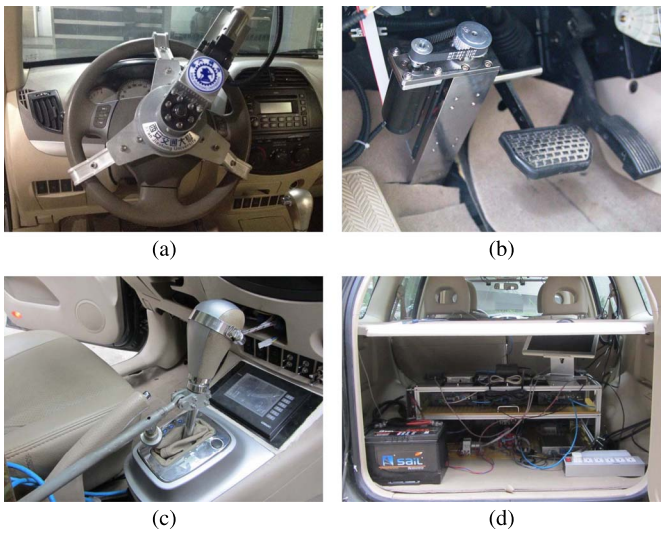

Fig. 8. Actuation and computing system design for controlling Kuafu-II vehicle, including (a) steering actuator, (b) brake and throttle actuators, (c) gear lever actuator, and (d) industrial PC in the trunk.

where steering wheel, brake and throttle pedal, gear lever are major modified actuators.

- Steering actuator: A dedicated mechanism (shown in Fig. 8(a)) controlled by a servo motor has been fixed on steering wheel directly. It can be supported either by windshield using a vacuum chuck or by handrail of the front doorframe using screws. On the load side, the mechanism is able to provide the torque that is not less than 8 Nm.
- Brake and acceleration pedal actuators: A linear motion mechanism (shown in Fig. 8(b)) has been installed as brake pedal actuator. On the load side, the force that is not less than 500 N can be provided by the mechanism; In addition, by employing engine management system of the vehicle, an analog output module is used to generate the control signal that originally comes from acceleration pedal.
- Gear lever actuator: Another linear motion mechanism (shown in Fig. 8(c)) has been installed as gear lever actuator. The mechanism has been carefully calibrated to precisely control for each gear.

Moreover, to guarantee the driving safety, all actuators are also designed to be easily overridden by human driver.

The software of the automatic driving control module has been implemented on industrial PC with the CPU of Intel Core i3-2310E. An dedicated thread has been assigned to execute longitudinal and lateral control algorithms. The control program is executed at a rate of 50 Hz, and is synchronized by either GPS time or special CAN package from vehicle ECU. The overall control program takes around 40% of the overall CPU time.

IV. Experimental Results

To demonstrate the performance of the designed automatic driving control system, both simulation tests and on road tests

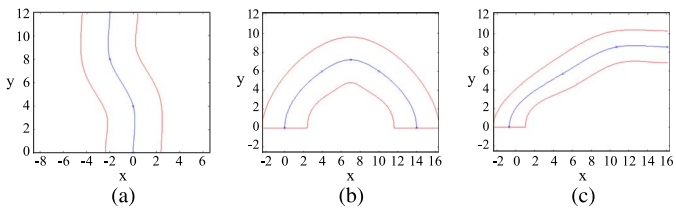

Fig. 9. Generated trajectory used for error calculation, including (a) obstacle avoidance trajectory, (b) U-turn trajectory, and (c) curve trajectory.

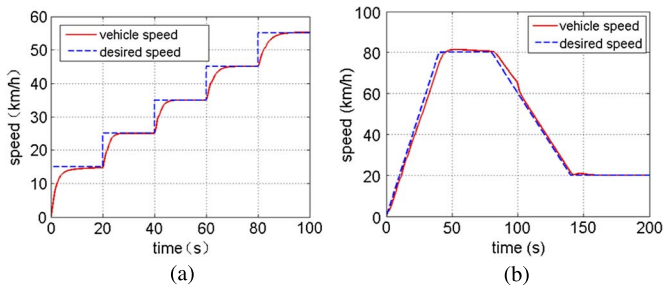

Fig. 10. Simulation results for the longitudinal control, including (a) step response and (b) ramp response.

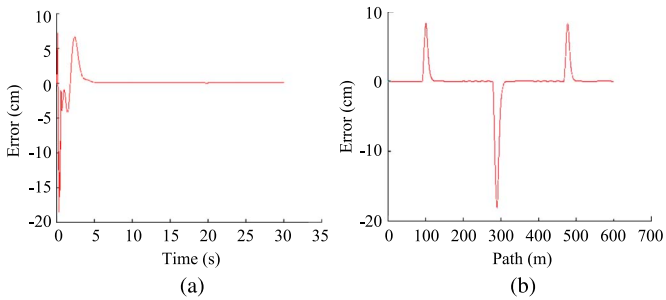

Fig. 11. Simulation results for the lateral control in case of (a) s-turn and (b) high curvature left turn.

in urban scenarios have been carried out. The autonomous vehicle uses parameterized cubic spline interpolation function to generate desired trajectory for the automatic driving control module. The generated trajectories for typical scenarios, including obstacle avoidance, U-turn and curve lane, are shown in Fig. 9.

To evaluate the performance of longitudinal control, we elaborate the simulation by using the vehicle model from [20]. Fig. 10(a) shows the step response of longitudinal controller. Taking ride comfort into consideration, the pole of the reference model is selected to get a relatively slow transient. A series of step response experiments have been taken using the magnitude of 10 km/h. Similar transient response has been presented at different operating points from low speed to high speed, and all the steady-state errors are zeros. Fig. 10(b) depicts speed profile tracking performance by ramp response. The speed profile has a 0 to 80 km/h acceleration ramp and a 80 to 20 km/h deceleration ramp. The steady-state error following the ramp signal is small enough in all the speed range.

For lateral control, some driving course are used to test attributes of lateral controller. Fig. 11 shows the simulated

Fig. 12. Bird's eye view of the test spot from Google Map.

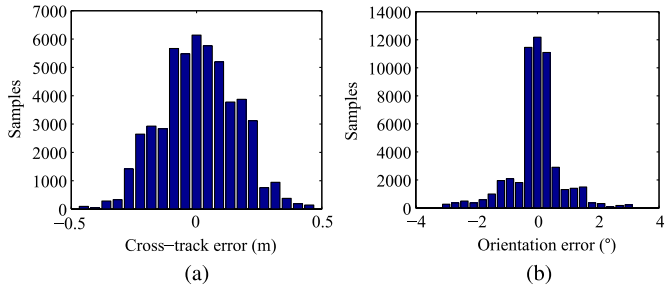

Fig. 13. Crosstrack and Orientation error histograms of the presented track in Fig. 12.

Fig. 14. The rural course of IVFC'2012, which is featured with large undulating roadbed and small curvature curve road (a) and located on the western fringes of Horqin sandy land (b).

error $e_o \approx e_1 + de_2$ that combines both cross-track error and orientation error when taking two courses. Fig. 11(a) shows the error for the curvature step course from a straight path to a constant nonzero curvature path, Fig. 11(b) shows the error for the S-shape course. We can see from simulation result that steady-state error is zero, and transient error is also very small whose its magnitude is less than 0.2 m.

In addition to simulation, we also evaluate the described driving control system by on road test. Fig. 12 shows the bird's eye view of one of the test spots from Google Map. The trial path is chosen due to its variable curvatures, which enables an appropriate prototyping evaluation. Moreover, the test track is along the riverside that is a relatively open field, which can minimize the multipath. By setting the base-station at the center of the spot, which can provide the best data-link radio, the real-time kinematic(RTK) differential GPS can provide a position precision which is less than 5 cm. Before the test, the track path has been sampled by using a RTK GPS and inertial measurement system installed on the vehicle. The dense data of sampled position have been processed into desired GPS waypoints offline. the GPS waypoints space about 10 m. A cubic spline defined by sequential four waypoints is used as desired track path that guarantees the continuous and smooth, and can been executed by the vehicle. The waypoints at turn corner should be selected carefully. In the test, the position of the vehicle can been measured by GPS and inertial measurement system, the distance to the cubic spline is the crosstrack error and the angle from the tangent line at the nearest point on the curve to the orientation of the vehicle is the orientation error. The crosstrack and orientation error histogram in one trial is illustrated in Fig. 13, where a speed profile with the maximum speed of 60 km/h has been set for the trial. We can see that, the maximum crosstrack error is less than 0.5 m, and the great majority of crosstrack errors are less than 0.2 m.

V. Evaluation in Future Challenge Competitions

Since 2009, National Natural Science Foundation of China (NSFC) has initiated and organized a series of competitions, named Intelligent Vehicle Future Challenge (IVFC), to promote the research about the ability of computer's perception to natural environment and intelligent decision-making. IVFC has attracted much attention in China and abroad and more than ten teams take part in the competition each year [21], [22]. Equipped with the presented driving control system, Kuafu-II autonomous vehicle has participated in IVFC'2012 and IVFC'2013. In the competition, the driving control system demonstrated its high availability and reliability under diversified circumstance.

IVFC'2012 was held on October 31, 2012 in Ongniud Qi, Inner Mongolia Autonomous Region. The competition consisted of two separate courses, one for urban environment, the other for rural environment. In particular, the rural course was located on the western fringes of Horqin sandy land, which was featured with large undulating roadbed and small curvature curve as shown in Fig. 14. Kuafu-II autonomous vehicle equipped with the described driving control module presented excellent performance on these scenarios and won the second prize in IVFC'2012.

IVFC'2013 was held in Changshu, Jiangsu Province on November 2, 2013. The competition also included rural road course (Fig. 15(a)) and city road course (Fig. 15(b)). The rural road course was around Kuncheng Lake and took about 18 km. Different from the rural course of IVFC'2012, this rural course was featured with small undulating roadbed and large curvature curve. Due to the existence of quite a few sharp curves, the performance monitor in the automatic driving control module tended to make Kuafu-II slow down rapidly and speed up slowly. This caused the speed of Kuafu-II autonomous vehicle was relatively slow on the rural road. In addition, we

(a) (b)

Fig. 15. Two race courses in IVFC'2013: (a) the rural course and (b) the city course.

deliberately traded-off maneuverability of Kuafu-II autonomous vehicle for enhanced safety, by giving longitudinal regulation high priority and restricting steering magnitude. These even caused the vehicle get stuck twice due to the false alarms of obstacle detection. Nevertheless, Kuafu-II autonomous vehicle still completed all the required courses and showed robust performance in IVFC'2013.

The control structure of Kuafu-II autonomous vehicle is designed conservatively to guarantee the safety for real-road test. Although the research on autonomous maneuver behaviors has attracted increasing attention, how to determine the optimal trade-off between maneuverability and safety in autonomous vehicle is still a grand challenge. To further address this problem and increase maneuverability may require cross-layer exploration among environmental perception, decision making and planning, and driving control system.

VI. Conclusion

This paper presents the design of driving control system for Kuafu-II autonomous vehicle, which is developed as a testing platform for robotic perception, decision and planning. The driving control system consists of both longitudinal and lateral controllers, where several adaptive and robust control algorithms have been integrated to improve compatibility and minimize calibration overhead. The presented driving control system can guarantee the autonomous vehicle is controlled fully at slow speed and in small signal range at high speed. The overall control system has been implemented on an industrial PC and integrated into Kuafu-II autonomous vehicle, and its performance is evaluated by simulation and on road test.

References

[1] M. Buehler, K. Iagnemma, and S. Singh, Eds., *The 2005 DARPA Grand Challenge: The Great Robot Race*. Berlin, Germany: Springer-Verlag, 2007.

[2] M. Buehler, K. Iagnemma, and S. Singh, *The DARPA Urban Challenge: Autonomous Vehicles in City Traffic*. Berlin, Germany: Springer-Verlag, 2009.

[3] J. Xin, C. Wang, Z. Zhang, and N. Zheng, "China future challenge: Beyond the intelligent vehicle," *IEEE Intell. Transp. Syst. Soc. Newslett.*, vol. 16, no. 2, pp. 8–10, Apr. 2014.

[4] S. Thrun *et al.*, "Stanley: The robot that won the DARPA grand challenge," *J. Field Robot.*, vol. 23, no. 9, pp. 661–692, Sep. 2006.

[5] C. Urmson *et al.*, "Autonomous driving in urban environments: Boss and the urban challenge," *J. Field Robot.*, vol. 25, no. 8, pp. 425–466, Aug. 2008.

[6] Y. Chen *et al.*, "TerraMax: Team Oshkosh urban robot," *J. Field Robot.*, vol. 25, no. 10, pp. 841–860, Oct. 2008.

[7] R. E. Fenton and R. J. Mayhan, "Automated highway studies at the Ohio State University—An overview," *IEEE Trans. Veh. Technol.*, vol. 40, no. 1, pp. 100–113, Feb. 1991.

[8] P. Ioannou, Z. Xu, S. Eckert, D. Clemons, and T. Sieja, "Intelligent cruise control: Theory and experiment," in *Proc. IEEE Conf. Decision Control*, 1993, pp. 1885–1890.

[9] P. Hingwe and M. Tomizuka, "Experimental evaluation of a chatter free sliding mode control for lateral control in AHS," in *Proc. Amer. Control Conf.*, 1997, pp. 3365–3369.

[10] J. Hedrick, M. Tomizuka, and P. Varaiya, "Control issues in automated highway systems," *IEEE Control Syst.*, vol. 14, no. 6, pp. 21–32, Dec. 1994.

[11] J. E. Naranjo, C. Gonzlez, R. Garcła, and T. de Pedro, "Using fuzzy logic in automated vehicle control," *IEEE Intell. Syst.*, vol. 22, no. 1, pp. 36–45, Jan./Feb. 2007.

[12] J. Prez, V. Milans, and E. Onieva, "Cascade architecture for lateral control in autonomous vehicles," *IEEE Trans. Intell. Transp. Syst.*, vol. 12, no. 1, pp. 73–82, Mar. 2011.

[13] R. Attia, R. Orjuela, and M. Basset, "Coupled longitudinal and lateral control strategy improving lateral stability for autonomous vehicle," in *Proc. Amer. Control Conf.*, 2012, pp. 6509–6514.

[14] A. Katriniok, J. P. Maschuw, F. Christen, L. Eckstein, and D. Abel, "Optimal vehicle dynamics control for combined longitudinal and lateral autonomous vehicle guidance," in *Proc. Eur. Control Conf.*, 2013, pp. 974–979.

[15] A. Broggi, P. Medici, P. Zani, A. Coati, and M. Panciroli, "Autonomous vehicles control in the VisLab intercontinental autonomous challenge," *Annu. Rev. Control*, vol. 36, no. 1, pp. 161–171, Apr. 2012.

[16] C. M. Filho, D. F. Wolf, V. G., Jr., and F. S. Osorio, "Longitudinal and lateral control for autonomous ground vehicles," in *Proc. IEEE Intell. Veh. Symp.*, 2014, pp. 588–593.

[17] J. Funke *et al.*, "Up to the limits: Autonomous Audi TTS," in *Proc. IEEE Intell. Veh. Symp.*, Jun. 2012, pp. 541–547.

[18] A. H. Glattfelder, W. Schaufelberger, and H. Fassler, "Stability of override control systems," *Int. J. Control*, vol. 37, no. 5, pp. 1023–1037, May 1983.

[19] A. M. Foss, "Criterion to assess stability of a 'lowest wins' control strategy," *Proc. Inst. Elect. Eng. D—Control Theory Appl.*, vol. 127, no. 1, pp. 1–8, Jan. 1981.

[20] H. Ohtsuka and L. Vlacic, "Stop & go vehicle longitudinal model," in *Proc. IEEE Int. Conf. Intell. Transp. Syst.*, Sep. 2002, pp. 206–209.

[21] Y. Jiang *et al.*, "Design of a universal self-driving system for urban scenarios—BIT-III in the 2011 Intelligent Vehicle Future Challenge," in *Proc. IEEE Intell. Veh. Symp.*, 2012, pp. 506–510.

[22] T. Mei *et al.*, "Development of 'Intelligent Pioneer' unmanned vehicle," in *Proc. IEEE Intell. Veh. Symp.*, 2012, pp. 938–943.

Linhai Xu received the bachelor's degree from the Shaanxi University of Technology, Hanzhong, China, in 1993 and the M.S. degree from Xi'an Jiaotong University, Xi'an, Shaanxi, China, in 2001. In 1993, he joined Xi'an Jiaotong University, where he is currently an Engineer with the Institute of Artificial Intelligence and Robotics, Xi'an Jiaotong University. His current research interests include intelligence systems, robot vision, and industrial automation.

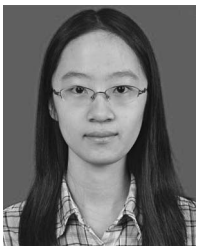

Yingzhou Wang received the bachelor's degree from Xi'an Jiaotong University, Xi'an, China, in 2013. She is currently working toward the M.S. degree with the Institute of Artificial Intelligence and Robotics, Xi'an Jiaotong University. Her main research interests include intelligence systems and pattern recognition.

Hongbin Sun (M'11) received the B.S. and Ph.D. degrees in electrical engineering from Xi'an Jiaotong University, Xi'an, China, in 2003 and 2009, respectively. From 2007 to 2008, he was a Visiting Ph.D. Student in electrical, computer, and systems engineering with Rensselaer Polytechnic Institute, Troy, NY, USA. From 2009 to 2011, he was a Postdoctoral Researcher with the Department of Computer Science, Xi'an Jiaotong University. He is currently an Associate Professor with the School of Electronic and Information Engineering, Xi'an Jiaotong University. His current research interests include memory hierarchy in computer system, VLSI architecture for video processing and computer vision, and signal processing system for new memory technology.

Jingmin Xin (S'92–M'96–SM'06) received the B.E. degree in information and control engineering from Xi'an Jiaotong University, Xi'an, China, in 1988 and the M.S. and Ph.D. degrees in electrical engineering from Keio University, Yokohama, Japan, in 1993 and 1996, respectively.

From 1988 to 1990, he was with the Tenth Institute of Ministry of Posts and Telecommunications (MPT) of China, Xi'an. He was with the Communications Research Laboratory, MPT of Japan, as an Invited Research Fellow of the Telecommunications Advancement Organization of Japan, from 1996 to 1997, and as a Postdoctoral Fellow of the Japan Science and Technology Corporation, from 1997 to 1999. He was also a Guest (Senior) Researcher with YRP Mobile Telecommunications Key Technology Research Laboratories Company, Ltd., Yokosuka, Japan, from 1999 to 2001. From 2002 to 2007, he was with Fujitsu Laboratories Ltd., Yokosuka. Since 2007, he has been a Professor with Xi'an Jiaotong University. His research interests are in the areas of adaptive filtering, statistical and array signal processing, system identification, and pattern recognition.

Nanning Zheng (SM'93–F'06) graduated from the Department of Electrical Engineering, and the M.S. degree in information and control engineering from Xi'an Jiaotong University, Xi'an, China, in 1975 and 1981, respectively, and the Ph.D. degree in electrical engineering from Keio University, Yokohama, Japan, in 1985.

In 1975, he joined Xi'an Jiaotong University, where he is currently a Professor and the Director of the Institute of Artificial Intelligence and Robotics. His research interests include computer vision, pattern recognition and image processing, and hardware implementation of intelligent systems.

Dr. Zheng became a member of the Chinese Academy of Engineering in 1999, and he is the Chinese Representative on the Governing Board of the International Association for Pattern Recognition. He also serves as the President of Chinese Association of Automation.